Full-Wave Comparison of Z-cut and X-cut Lithium Niobate (LiNbO₃) Electrooptic Modulators Using Finite Element Method

T. Gorman and S. Haxha

Abstract: **In this study we compare the relative merits of Z-cut and X-cut lithium niobate (LN) electrooptic modulators. The finite element method (FEM) has been used to implement a full wave analysis of the two structures and determine the microwave effective index N_m, the characteristic impedance Z_c, the microwave losses α_c and the half wave voltage $V_\pi L$, operating at frequency range from 0.1 to 100GHz. Modelling of the diffusion profile of the optical waveguides has also been presented. The aim of the comparison of the two devices was to determine which device exhibit lower drive voltage at a high frequency operation.**

Index Terms—**Electrooptic modulators, communication systems, drive voltage, conductor loss.**

I. INTRODUCTION

Imperative for the communication industry to continue its transition into the next generation of ultra-high-speed communications is the development of low chirp, low drive power and high bandwidth external modulators. Mach-Zehnder (MZ) devices designed from either Z-cut or X-cut LN are the most common external modulators in operation today, operating at frequencies between 10 and 40GHz. Modulators based on Z-cut configuration have often been favoured as it is a relatively simple task to simultaneously match the microwave and optical signals and the characteristic impedance by increasing the buffer layer thickness between electrode and LN substrate. However this comes at the cost of increased drive voltage. Modulators based on the X-cut configuration do not necessarily require a buffer layer since the optical waveguides are placed between the electrodes rather than directly under them. Thus, optical absorption losses are not an issue here. Removal of the buffer layer allows for more of the modulating electric field to penetrate into the waveguide thereby increasing the electrooptic effect and consequently reducing the drive voltage. However the removal of the buffer layer means that velocity and impedance matching is made much more difficult and usually results in narrow electrode gaps and narrow bandwidths. A further advantage of X-cut LiNbO₃ modulators is that due to their symmetry the chirp is very low.

In this study, the finite element method (FEM) has been chosen as the simulation tool for the modulators since it is a well proven technology in this field and is capable of solving for the eigenvalues of complex topologies with features such as angled waveguides and electrodes and anisotropic structure of materials. A full wave-analysis is undertaken in order to determine the effects of frequency on the modulators microwave effective index, N_m characteristic impedance, Z_c conductor loss, α_c and half-voltage length-product, $V_\pi L$ which is not possible using the typical quasi-TEM analysis. The full-wave analysis is used to solve for the propagation constant rather than the structures capacitance as is the case with the quasi-TEM approximation.

The X-cut and Z-cut electrooptic modulators considered in this study are illustrated in Fig.1 and 2, respectively.
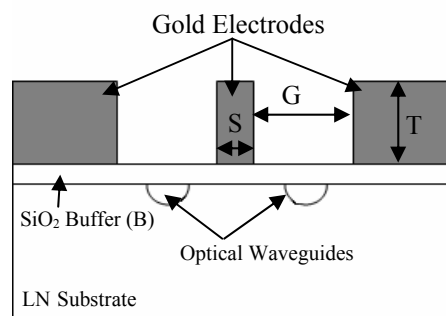

Fig. 1. X-Cut LiNbO₃ Modulator

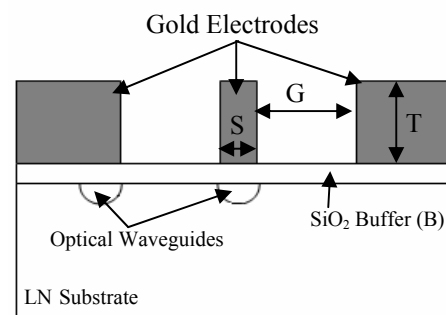
Fig. 2. Z-Cut LiNbO₃ Modulator

For the purpose of this simulation, the topology of both devices is identical with the exception of the positioning of the waveguides and the orientation of the crystal cut. The buffer layer B is 0.6μm, the electrode gap G is 25μm, the central 'hot' electrode width S is 8 μm and the electrode height T is varied between 10 and 29μm.

II. THEORY

A. Microwave Analysis

The FEM is used in order to undertake a full-wave analysis of the two devices, it is capable of dealing with complex structures with anisotropic characteristics such as found with LN. Maxwell's wave equation when considering the anisotropy of materials becomes:

$$\nabla \times E = -\mu \frac{\partial H}{\partial t} \qquad (1)$$

$$\nabla \times H = \sigma E + \overline{\overline{\varepsilon}} \frac{\partial E}{\partial t} \qquad (2)$$

where

$$\overline{\overline{\varepsilon}} = \begin{bmatrix} \varepsilon x & 0 & 0 \\ 0 & \varepsilon y & 0 \\ 0 & 0 & \varepsilon z \end{bmatrix} \qquad (3)$$

$\overline{\overline{\varepsilon}}$ is the diagonal relative permittivity tensors and E and H are the electric and magnetic fields.

In order to determine the microwave effective index N_m it is necessary to solve the above equations for the eigenvalues of the fundamental mode using the FEM. The microwave effective index can be calculated from:

$$N_m = \frac{\beta}{k_0} \qquad (4)$$

where β is the microwave propagation constant and k_0 is the free-space wave number which can be expressed as:

$$k_0 = \frac{2\pi}{\lambda} \qquad (5)$$

In order to determine the characteristic impedance of the devices we use the power-current definition:

$$Z_c = \frac{2P}{|I|^2} \qquad (6)$$

where P is the modal power and I is the current in the z-direction. The modal power P can be determined by solving the Poynting vector:

$$P = \frac{1}{2} \iint (E \times H^*) \cdot \mathbf{i_z} \cdot dxdy \qquad (7)$$

Where * denotes the complex conjugate and $\mathbf{i_z}$ is the unit vector in the z-direction. The integration is carried out over the entire waveguide cross section. The current in the z-direction can be determined by:

$$I = \iint \sigma E z \cdot dxdy \qquad (8)$$

Where σ is the electrode conductivity which for gold is equal to 4.1×10^7 S/m and the integration is carried out only over the central 'hot' electrode.

B. Optical Analysis

In order to determine the half wave voltage length product $V_\pi L$ it is necessary to solve for the fundamental optical mode of the device under the influence of an applied microwave electric field. The value of $V_\pi L$ can then be determined by [1, 2]:

$$V_\pi L = \frac{\pi V_0}{\Delta\beta} \qquad (9)$$

where $\Delta\beta = \beta_1 - \beta_0$ and β_1 and β_0 are the propagation constants of the fundamental mode of the Mach-Zehnder arms with and without the applied voltage respectively and V_0 is the applied voltage.

When considering the push-pull effect of the coplanar waveguide we need to consider the change in the propagation constant with respect to both waveguides, since for both X and Z-cut devices the propagation constant is increased in one arm of the guide whilst it is decreased in the other due to the polarity of the applied microwave electric field and the electrooptic effect of the LN waveguide.

In order to determine the frequency dependent drive voltage as a function of frequency $V\pi(f)$ the following expression is used:

$$V\pi(f) = V\pi(dc)10^{-m(f)/10} \qquad (10)$$

where the optical response $m(f)$ is measured in dB optical and the value of $V_\pi(dc)$ is determined by the value of V_π calculated from equation (9).

The optical response is calculated by the following [3]:

$$\left| \frac{1 - S_1 S_2}{(1 + S_2)[\exp(j2u+) - S_1 S_2 \exp(-j2u-)]} \times \left[\exp(ju+)\frac{\sin u+}{u+} + S_2 \exp(-ju-)\sin\frac{u-}{u-} \right] \right| \qquad (11)$$

Where

$$S_1 = \frac{Z_1 - Z}{Z_1 + Z} \quad S_2 = \frac{Z_2 - Z}{Z_2 + Z} \qquad (12)$$

and

$$u_-^+ = \frac{1}{c}\pi f l(N_m \mp N_{eff}) - j\frac{1}{2}\alpha_c l \qquad (13)$$

with Z, Z_1 and Z_2 being the microwave characteristic impedance, the microwave generator internal impedance and the shunted load impedance respectively, c is the speed of light, f is the microwave frequency, l is the electrode interaction length, N_m is the microwave effective index, N_{eff} is the optical effective index and α_c is the microwave attenuation constant.

III.   RESULTS and DISCUSSIONS

C. Microwave analysis

We first consider the microwave characteristics of the two modulators, Z-cut and X-cut. In the microwave region the relative permittivity tensor is as discussed in (3) with the permittivity of the LN substrate being 28 in extraordinary axes and 43 in the two ordinary axes. The permittivity of the silicon dioxide (SiO_2) buffer layer is 3.9 and the conductivity of the gold electrodes is 4.1×10^7 S/m. When calculating the optical response we assume that $Z_1 = Z_2 = 50\Omega$ and that N_{eff} of the unmodulated LN waveguide is 2.142. We also set the electrode interaction length to 1cm. First we have investigated the microwave index N_m and microwave loss as a function of frequency for the two devices with the electrode height T = 29μm:
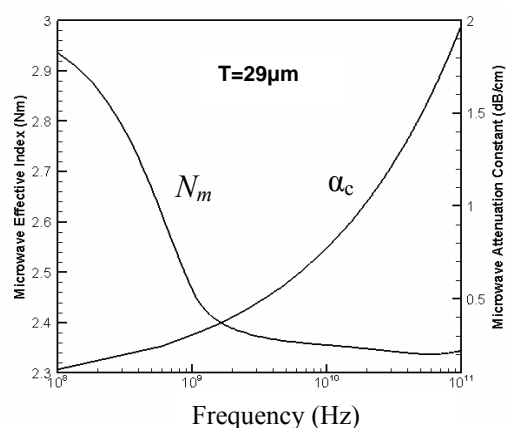

Fig. 3. Variation of microwave effective Index N_m and attenuation constant α_c as a function of frequency for Z-cut configuration, when T = 29μm.

Clearly both parameters vary significantly with frequency. In particular a significant increase in the attenuation constant can be observed at high frequency operation. The value of N_m decreases rapidly over the first decade up to around 1GHz and then converges to a value of around 2.34 at 100GHz.
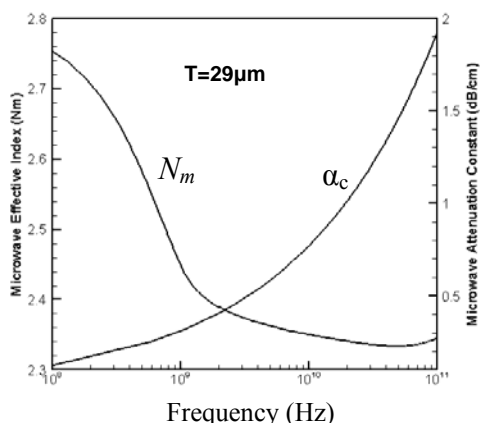

Fig. 4. Variation of microwave effective Index N_m and attenuation constant α_c as a function of frequency for X-cut configuration, when T = 29μm.

Next we have investigated the same parameters for the X-cut configuration. A similar behaviour of the X-cut is observed and is shown in Fig. 4. This confirms that at a high operating frequency, both the Z-cut and X-cut modulators exhibit similar performance.

The frequency dispersion of N_m and α_c are almost identical for both Z-cut and X-cut devices, with a slightly lower value of N_m and α_c for the X-cut device across the frequency range. Next investigation of the characteristic impedance of the two modulators is carried out.
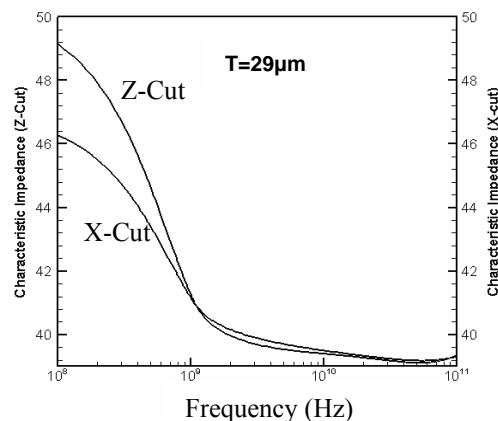

Fig. 5. Variation of characteristic impedance as a function of frequency for Z-cut and X-cut configuration, when T = 29μm.

Clearly the X-cut device has a lower Z_c at frequencies below 1GHz; however at frequencies above 1GHz the values of Z_c are similar, converging to a value of around 39Ω. The characteristic impedance of the two devices is clearly frequency dependent especially at frequencies below 1GHz. This effect can be attributed to the finite value of the electrode conductivity. At low frequencies the increase in Z_c can be attributed to the increase in L and R/(ωL)[4] where R and L are the equivalent line resistance and inductance respectively.

By inspection of the graphs above it is clear that neither device is matched to the desired value of Z_c=50Ω and the desired value of N_m=2.142 required in order to maximise bandwidth. From previous work [3] it is known that reducing the height of the electrode increases the value of Z_c whilst at the same time increasing the value of N_m. It is also known that increasing the buffer layer thickness increases the value of Z_c whilst at the same time reducing the value of N_m. The following figures show the effects of reducing the height of the electrodes to 10μm.
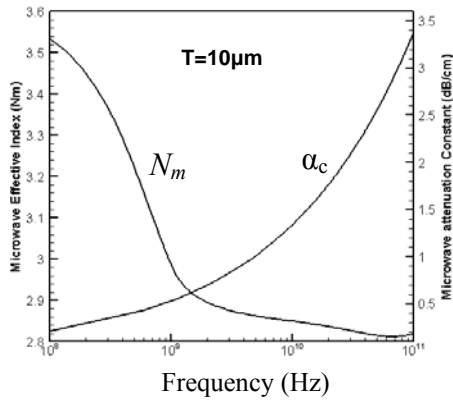
Fig. 6. Variation of N_m and α_c as a function of frequency for Z-cut configuration when T = 10μm.

For the Z-cut configuration, when the electrode height is reduced to 10μm, the value of N_m is increased by around 27% from 2.75 when the electrode height was 29μm, to around 3.5. Again the rate of change in N_m is greatest below around 1GHz. N_m then converges to a value of around 2.8 at 100GHz. The microwave attenuation constant increases by around 3.5dB across the frequency range.
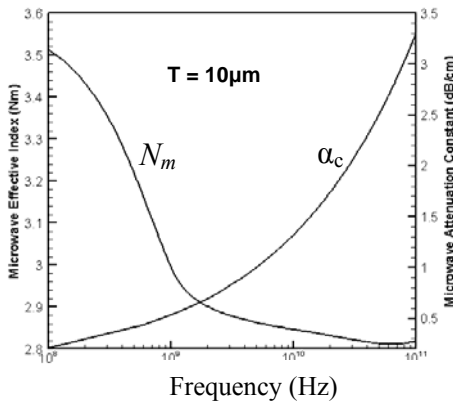

Fig. 7. Variation of N_m and α_c as a function of frequency for X-cut configuration when T = 10μm.

For the X-cut device we observe a similar trend, when the electrode height is reduced the value of N_m increases and so does the attenuation constant. Clearly for a low microwave loss device a thicker electrode is desirable though this inevitably results in an increase in N_m.
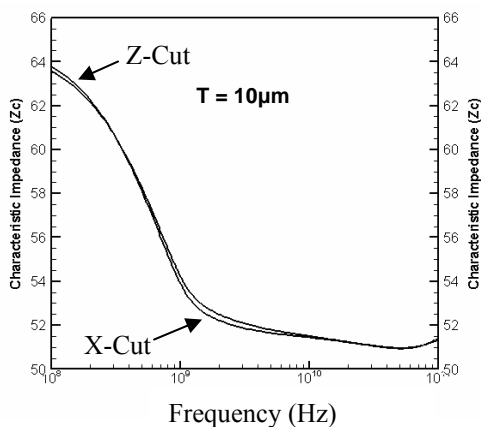

Fig. 8. Variation of characteristic impedance as a function of frequency for Z-cut and X-cut configuration when T = 10μm.

Fig. 8 presents the characteristic impedance Z_c for both configurations when T = 10μm.
With respect to both devices the value of Z_c has increased significantly, however at higher frequencies the value of Z_c is much closer to the desired value of 50Ω.
Clearly in order to produce an optimised device whereby the value of N_m and Z_c are simultaneously matched to that of the optical effective index and the impedance of the microwave generator requires that we consider the effects of frequency dispersion on the modulators performance.

D. Optical analysis

Next investigation of the optical properties of the two modulators is carried out. At optical wavelength 1.55μm the refractive index of the LN substrate is around 2.214 with respect to the ordinary optical axes and around 2.138 for the extraordinary. The waveguides are generally formed by titanium indiffusion which increases the refractive index slightly in the waveguide region. The increased refractive index contour is modelled using the following well documented equations [5]:

$$n_o = n_{os} + \Delta n_o \left[f(x)g(y) \right]^{0.55} \tag{14}$$

$$n_e = n_{es} + \Delta n_e \left[f(x)g(y) \right] \tag{15}$$

Where

$$f(x) = \frac{erf\left(\frac{2x+W}{2dx} \right) - erf\left(\frac{2x-W}{2dx} \right)}{2erf\left(\frac{W}{2dx} \right)} \tag{16}$$

and

$$g(y) = \exp\left[-\left(\frac{y}{dy} \right)^2 \right] \tag{17}$$

where n_{os} and n_{es} are the ordinary and extraordinary refractive indexes of LN and Δn_o and Δn_e are the maximum ordinary and extraordinary refractive index changes. W is the width of the titanium strip before indiffusion, d_x and d_y are the diffusion lengths in the x and y directions, respectively. The values for Δn_o and Δn_e were taken as 0.0062 and 0.0146 respectively and W=0.6μm. The value of $dx = 4.85$μm and $dy = 4.105$μm.

The refractive index of the SiO_2 buffer layer was taken as 1.45 and the complex refractive index of the gold electrodes was taken to be 0.379-j10.75. Fig. 9 shows a typical contour plot of the fundamental H_{11} mode.
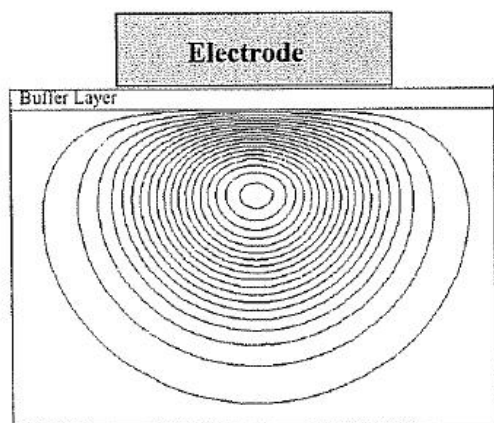
Fig. 9. Contour plot of fundamental H_{11} mode. Z-cut configuration.

Fig 9 shows that the mode is more tightly confined where the induced change in refractive index is the strongest, evident by the tighter contours nearest to the electrode and less so where the microwave electric field is at its weakest at the extremities of the mode contour. The compressed, spherical shape of the mode is also evidence that the diffusion model is also operating correctly since the highest change in refractive index, caused by the indiffusion process, is directly beneath the centre of the electrode, reducing as the distance increases from this point in the x and y directions.

In order to calculate the frequency dependence of the drive voltage we determine $V_\pi(dc)$ by using (9) then use (10) to determine the frequency response of the drive voltage. The results are presented in Fig. 10 and 11.
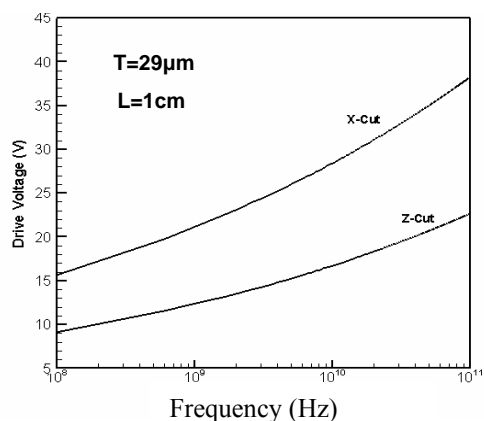

Fig. 10. Variation of drive voltage as a function of frequency for Z-cut and X-cut configuration when T = 29μm.

For the Z-cut modulator with T = 29μm the drive voltage is around 9V at the low end of the frequency scale, rising to around 23V at the high end, a significant increase of around 150%. For the X-cut device the drive voltage is significantly higher at around 16V at the low end to around 38V at the higher, an increase of around 138% across the frequency range.
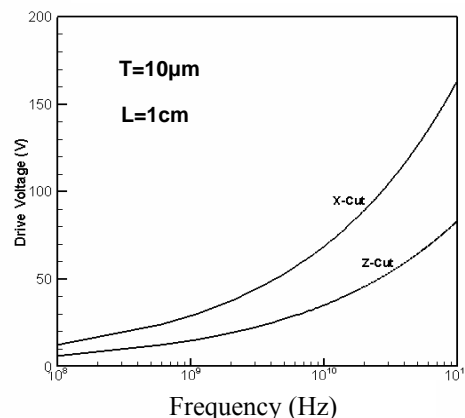

Fig. 11. Variation of drive voltage as a function of frequency for Z-cut and X-cut configuration when T = 10μm.

When the electrode height is reduced to 10μm there is a significant rise in the drive voltage. For the Z-cut device, at the low end of the frequency range, the drive voltage is again around 9V. However, at the upper end of the frequency range it has increased to around 80V, an increase of around 780% over the frequency range. For the X-cut device, again at the low end of the frequency range, the drive voltage is around 12V; however at the high end the drive voltage has increased to around 160V. As can be seen there is a significant increase over the frequency range.

The X-cut device has the higher value of drive voltage and this is no surprise since the electric field strength is reduced firstly by the buffer layer and secondly by the distance that the electrodes are from the active waveguide region (see Fig 1). In order to reduce the drive voltage of the X-cut device total or partial removal of the buffer layer would be required. Or alternatively the electrodes could be positioned closer together to increase the electric field strength around the waveguide. Both of these solutions have issues: firstly by removing the buffer layer the value of N_m is significantly reduced and secondly reducing the electrode gap is known to reduce the bandwidth. A further option is to use thin strip technology whereby a thin strip of LN is bound to a substrate of lower permittivity. Using this technique it is possible to remove the buffer layer completely and at the same time simultaneously match the microwave effective index to the optical effective index and the characteristic impedance of the device to the signal source generator.

IV. CONCLUSION

A full-wave analysis was applied to Z-cut and X-cut electrooptic modulators and the effects of frequency on the microwave effective index, characteristic impedance, attenuation constant and power consumption have been demonstrated. The diffusion profile of the modulator waveguides have also been modelled and presented. It has been demonstrated that the Z-cut device has the lowest value of $V_\pi L$ over the frequency range, however the X-cut devices performance may be significantly improved by the removal of the buffer layer and further investigation (currently underway) into thin film technology in order to improve simultaneous matching of N_m and Z_c.

REFERENCES

[1]. S. Haxha, B. M. A Rahman, R. J. Langley, "Broadband and Low-Driving power LiNbO$_3$ electrooptic modulators", *Optical and Quantum Electronics,* vol. 36, pp. 1205-1220, 2004

[2] B. M. A. Rahman and S.Haxha, "Optimisation of Microwave Properties for Ultrahigh-speed Etched and Unetched Lithium Niobate Electrooptic Modulators", *IEEE, J. Lightwave Technology*, vol. 20, No. 10, pp. 1856-1863, 2002.

[3]. S. Haxha, B. M. A. Rahman, and K.T.V.Grattan, "Bandwidth estimation for ultra-high-speed lithium niobate modulators", *Applied Optics*, Vol. 42, No. 15, pp. 2674-2682, 2003.

[4]. W. K Wang, R. W. Smith, P. J Anthony, "Full wave analysis of coplanar waveguides for LiNbO$_3$ optical modulators by the mode matching method considering nonideal conductors on etched buffer layers", *IEEE, J. Lightwave Technology*, vol. 13, pp. 2250-2257, 1995.

[5] E. Strake, G. P. Bava, I. Montrosset,"Guided modes of Ti:LiNbO$_3$ channel waveguides: A novel quasi-analytical technique in comparison with the scalar finite-element method" *IEEE, J. Lightwave Technology*, vol. 6, pp. 1126-1135, 1998.